

Nanoscale Arrangement of Proteins by Single-Molecule Cut-and-Paste

Mathias Strackharn,[‡] Diana A. Pippig,^{*,‡} Philipp Meyer, Stefan W. Stahl,[†] and Hermann E. Gaub

Center for Nanoscience and Department of Physics, University of Munich, Amalienstraße 54, 80799 Munich, Germany

S Supporting Information

ABSTRACT: Protein-based nanostructures are key to the organization of life and it is their precise arrangement, which determines their specific functions. A single-molecule approach for the directed assembly of protein arrangements allows for a controlled composition of systems based on protein components. Applying antibodies and antigenic peptide tags we utilized the Single-Molecule Cut-and-Paste (SMC&P) technique for the handling of single proteins. Protein–DNA complexes could be arranged to complex patterns with the functionality of the protein part remaining unimpaired.

The ability to arrange individual proteins in a controlled manner on a surface is a prerequisite for the study of complex systems, e.g. of enzyme networks as a function of composition and alignment. With the growing number of theoretical descriptions of biochemical networks,¹ the need for model systems, with a controllable set of parameters at the single-molecule level, arises to shed light onto the underlying processes. Due to their high spatial precision, AFM-based methods have been widely used in the past for creating adjustable nanopatterns of biomolecules on surfaces. Dip pen nanolithography, for instance, or enzyme-assisted AFM-based nanolithography provide simple means to write molecular patterns, e.g. protein arrays with dimensions in the tens of nanometer range.^{2–7} However, for the bottom-up assembly of complex, functional protein arrangements, higher accuracy and control over the individual molecule as well as versatility are desirable. With single-molecule cut-and-paste (SMC&P) we recently implemented a technique for one-by-one arrangement of molecules under physiological conditions.⁸ With this technique the bottom-up assembly of biomolecular structures from biological building blocks has already been demonstrated successfully in several examples. Utilizing attachment geometries resulting in different binding forces, single DNA molecules can be repeatedly picked up from a depot region by a functionalized AFM tip and then be placed with the precision of an AFM⁹ on a target surface. The accuracy of the molecular deposition process was shown to depend on the length of the cross-linker, which serves to couple the anchor DNA to the surface. For the current study, with positioning accuracy not being a main objective, we used a 5 kD PEG spacer, which was shown to provide a precision in the 10 nm range.¹⁰

Until today applications of this technique were solely realized by making use of a DNA-based hierarchical force system for pick up and deposition.^{11–13} To make the SMC&P technology

accessible to the field of protein science, an approach beyond mere DNA interactions is needed.

We recently established an alternative implementation of a hierarchical force system, which replaces the DNA handle interaction between the transfer molecule and the AFM tip by a peptide–antibody complex.¹⁴ Such an interaction is desirable for the transport of single proteins. A prerequisite for this is the construction of fusion proteins harboring small antigenic peptide tags, which serve as handles on the protein of interest. Thus, a fully expressible system is obtained that does not require any additional modification of the protein.

For a first realization of a molecule-by-molecule arrangement of proteins based on this force system, an engineered fusion construct consisting of a zinc finger¹⁵ and a GFP^{16,17} moiety was used (Figure 1), allowing for positioning with mechanical control. A single-chain antibody fragment that recognizes the 34 residue GCN4(7P14P) random coil peptide^{18,19} was employed as handle system. For anchoring the construct to depot and target site, DNA hybridization was utilized. Thus, a connection between protein moiety and the DNA anchors is required. To this aim we used a six zinc finger construct that contains the three-finger peptide Zif268 and its mutated variant, NRE,²⁰ separated by a flexible linker. Zif268/NRE binds sequence specifically and with a subpicomolar affinity to a 29-bp dsDNA.²¹ The GCN4–GFP–zinc finger fusion construct was expressed in *E. coli*. Purified protein was bound to a connection DNA harboring the zinc finger target sequence and a 70 nucleotide long overhang. This contains a 30 nt spacer and 40 nt stretch chosen such that it can hybridize with the anchor sequence in the depot and in the target area. In addition the connector DNA was labeled with a Cy5 dye.

Utilizing a microfluidics system²² mounted on a coverslip, we created a depot and a target site by functionalizing the glass surface with anchor DNAs. On the depot site these oligonucleotides were covalently attached at their 5' end, on the target site at the 3' end. Then the complex of the GCN4–GFP–zinc finger fusion protein with the connector DNA was hybridized to the depot anchors. The single-chain antibody fragments were covalently bound to the cantilever tip. For the cyclic transfer of the proteins to the target site (Figure 1) the cantilever is first lowered toward the depot area, where the antibody is allowed to bind to the GCN4 peptide tag of the protein construct. In retracting the cantilever, all bonds of the system are loaded with the same force in series. Since the hybridization bond to the anchor DNA is in unzip geometry,

Received: June 12, 2012

Published: September 5, 2012

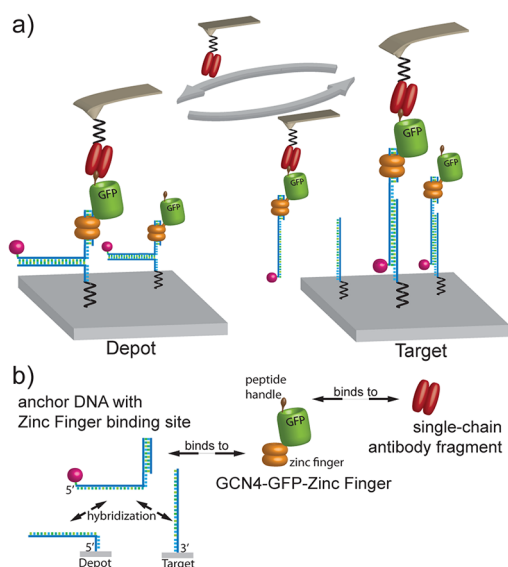


Figure 1. (a) Schematics of the transfer process. The GCN4–GFP–zinc finger construct is bound with high affinity to the anchor DNA and stored via hybridization in the depot area. A single-chain antibody fragment, which is covalently attached to the cantilever tip, seizes the GCN4-tag, and the DNA in unzip geometry opens up when the cantilever is lifted. The GCN4–GFP–zinc finger construct with the anchor DNA can then be transferred to the target site, where the shear geometry bond to the target DNA is stronger than the bond between antibody and GCN4 peptide. The protein construct is deposited in the target area, whereas the antibody on the cantilever is free again and can be reused in the next transfer cycle. (b) Toolbox for the protein transport. The GCN4–GFP–zinc finger fusion protein can specifically bind to the DNA anchor strand via the zinc finger domain at the C-terminus. The N-terminal GCN4 peptide tag serves as a handle to pick up the complex.

the DNA strands separate base pair after base pair at a very low rupture force of about 25 pN, while the protein–connector–DNA complex remains attached to the cantilever, since the unbinding force of the peptide–antibody complex exceeds 40 pN at the given force loading rates. The cantilever with the zinc finger–DNA complex can then be moved by an *xy*-piezo system with angstrom precision to a predefined position in the target area. When the cantilever is lowered again, the connector DNA hybridizes to the anchor DNA. By subsequent retraction of the cantilever the hybridization bond, in contrast to the depot process, is now loaded in shear geometry. Because in this geometry all base pairs of the double strand are loaded in parallel, the rupture forces for opening up the DNA duplex bond are in the range of 60 pN. Since the antibody–peptide complex is already broken up at forces of 40 pN,¹⁴ the protein construct is detached from the cantilever and remains bound to the designated position on the target site via its DNA anchor (Figure S1, SI). The antibody at the cantilever is thus free again and can be reused for the next cut-and-paste cycle. It should be noted that the damage to the cantilever functionalization, e.g. by unfolding of the antibody, is negligible, thus allowing for several thousands of repeated cycles. Due to its very high affinity, the zinc finger–DNA complex was stable during the transfer.²³

We were able to simultaneously follow the single-molecule transfer in force spectroscopy^{13,24} and fluorescence spectroscopy.²⁵ During each of these cut-and-paste steps we independently confirmed, by recording the force–distance

traces, that individual molecules were handled. Figure 2 shows a gallery of typical traces. In (a) the force plateau prior to rupture

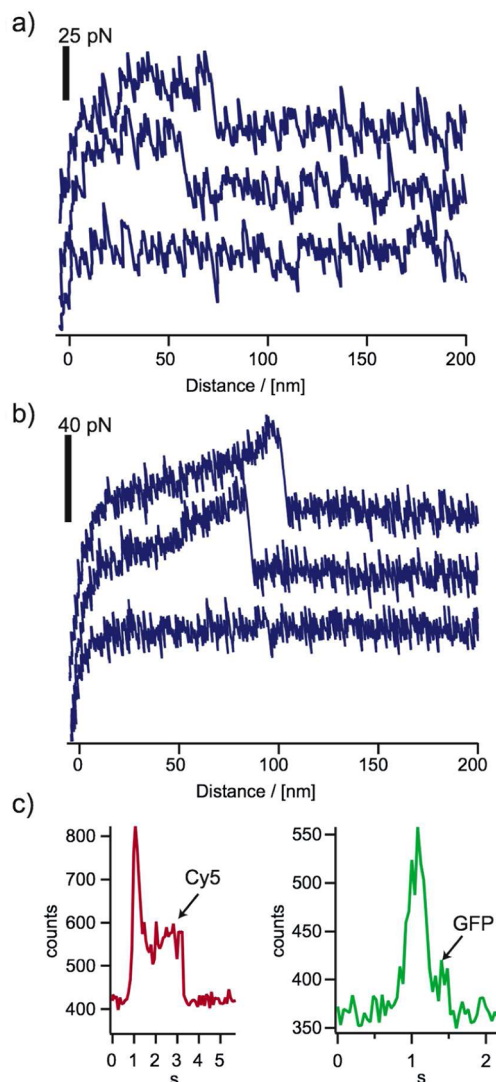


Figure 2. Typical force curves from (a) the depot region and (b) the target region. The cutting process in the depot region ends with a short plateau in the force–distance curve when the DNA is unzipped. When pasting the construct to the target area, the break of the antibody–antigen bond results in a sudden drop of the gradually built up force. In some cases no molecules were picked up or delivered, which is reflected in the zero-force curves. (c) The deposition process can be monitored in TIRF microscopy. Photons scattered from the cantilever and those emitted by the dye both contribute to the overall signal, when the cantilever enters the evanescent field. After the cantilever is retracted, fluorescence of the Cy5 (left) or GFP (right) remains until stepwise photobleaching occurs.

is characteristic for the unzipping of handle and anchor DNA, whereas in (b) the peak is typical for the all-or-none rupture of the antibody–peptide bond. The blank traces show that we were not able to pick up or deliver a molecule in all cases, which required a retry. Figure 2 (c) shows the time traces of a deposition process monitored in total internal reflection fluorescence from below. When the AFM tip with its zinc finger–DNA complex penetrates the evanescent field of the excitation laser, scattered light gives rise to the sharp increase, followed by the immediate drop when the tip is withdrawn. The

remaining fluorescence of the Cy5 label of the transfer DNA can now clearly be discerned against the background. It bleaches in a single step, proving at the given buffer conditions that we had indeed pasted an individual molecule. As was shown in previous studies, the position of this molecule can be determined with nanometer precision, given a sufficient photostability. The GFP signal of a pasted complex was monitored the same way. As it is well-known, the fluorophore lifetime of GFP is short. It has to be noted that the fluorophore is already exposed to the laser excitation while entering the evanescent field with the cantilever. Nevertheless, the fluorescence of the deposited GFP is clearly measurable, proving that the transfer process had not damaged the protein!

In order to demonstrate the robustness of the process, during 900 transport cycles the molecules were assembled to a micrometer-sized pattern of a red traffic light man.²⁶ The fluorescence of the Cy5 molecules could be imaged in objective-type TIRF microscopy²⁷ when excited with a red laser, albeit due to the Abbe-limited optics not in single-molecule resolution. The microscope was then switched to blue laser excitation and molecules were assembled to form the pattern of a green traffic light man. After the assembly the green emission of the GFP molecules was recorded. The results are shown in Figure 3. The two strongly fluorescing patterns prove the high reliability and robustness of this transport process. They also confirm that both the fusion protein, giving rise to

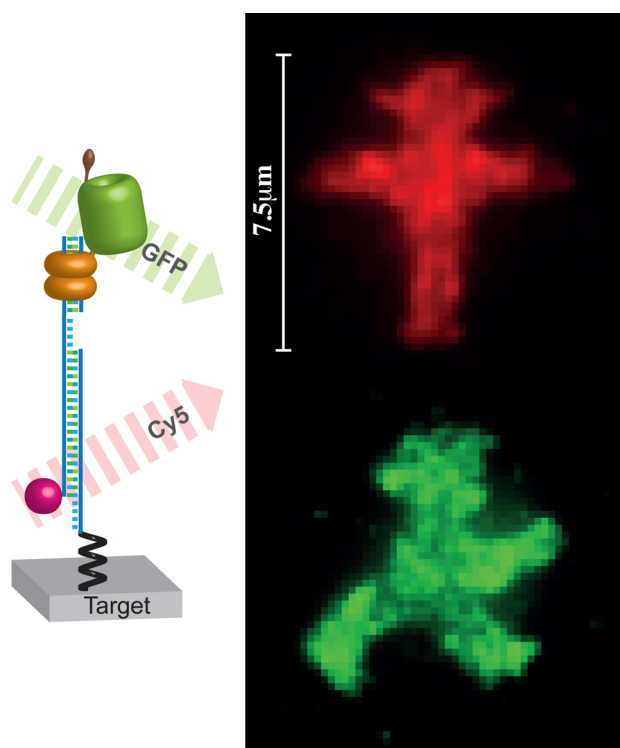


Figure 3. After 900 transport cycles of a protein–DNA construct a pattern displaying the red man of a pedestrian traffic light was assembled. The red emission of the Cy5 label at the DNA part was then measured. Next, the pattern of a green man was assembled, and this time the green fluorescence of the transferred GFP molecules was recorded. It proves that not only the cantilever-bound antibody fragment but also the transfer construct stays intact during the transfer cycles. The forces occurring during the transfer process are low enough so that the functionality of the transported GFP is not destroyed.

the GFP fluorescence, and the Cy5-labeled DNA are transported together. It should be noted that imperfections in the pattern arise from the varying functionalization densities in the depot and construction area but do not affect the conclusions drawn from this figure, that SMC&P of proteins is a feasible and robust process with negligible loss in transfer efficiency.

While the functionalization density of the involved molecules was chosen to result in an average transfer of two protein–DNA complexes per cycle (Figure S2, SI) it can be adjusted to yield varying transfer rates, as required for the respective application.

The critical components, when transferring and assembling proteins by SMC&P are the proteins that should be arranged and observed. Twice during the transfer process are forces applied to the GFP—first during the cut and again during the paste step. Forces are required to be low enough so as not to alter the structure of the protein and destroy its functionality. The fluorescence of the green traffic light man unambiguously proves that the GFP is still functional. The highest mean force that occurs during an SMC&P cycle arises as the antibody–antigen bond breaks. This force was set to be below 40 pN. Thus, the hierarchical force system is gentle enough for the transfer of proteins that do not undergo serious conformational changes before this value is reached. GFP was reported to open the barrel structure only at a force of around 100 pN.²⁸ Destruction should therefore not be expected.

Protein SMC&P harbors several advantages over established protein deposition methods. It offers an extremely high spatial resolution, around 10 nm, that is merely limited by the length of the spacers¹⁰ used for functionalization. While the mechanical control over the deposition process is key to this accuracy, it is importantly also used as a readout. The adjustability of the number of transport events by means of the surface functionalization density allows for versatile applications. Writing protein arrays containing several molecules of each species is possible as well as the precise deposition of a single protein, e.g. in the center of a zero mode waveguide.²⁹

This proof of concept provides a technological approach, which will allow for the assembly of networks from arbitrary protein constituents. Systems which develop new functionalities depending on their arrangement^{30,31} can be designed and studied with respect to composition and alignment. Also the assembly of enzyme cascades will become possible and may be studied by means of single-molecule fluorescence techniques. In combination with theoretical modeling this will provide for new insights into the cooperativity, stochastics, and kinetics underlying enzymatic reactions and signaling cascades.^{32–34}

■ ASSOCIATED CONTENT

📄 Supporting Information

Measurement details, preparation of proteins, surface chemistry, and oligonucleotide sequences. This material is available free of charge via the Internet at <http://pubs.acs.org>.

■ AUTHOR INFORMATION

Corresponding Author

diana.pippig@physik.uni-muenchen.de

Present Address

[†]Center for Integrated Protein Science (CIPSM), Munich, Germany.

Author Contributions

‡These authors contributed equally to this work.

Notes

The authors declare no competing financial interest.

ACKNOWLEDGMENTS

This work was supported by SFB 863 and the ERC.

REFERENCES

- (1) Armbruster, D.; Nagy, J. D.; van de Rijt, E. A.; Rooda, J. E. *J. Phys. Chem. B* **2009**, *113*, 5537.
- (2) Jaschke, M.; Butt, H. J.; Manne, S.; Gaub, H. E.; Hasemann, O.; Krimphove, F.; Wolff, E. K. *Biosens. Bioelectron.* **1996**, *11*, 601.
- (3) Piner, R. D.; Zhu, J.; Xu, F.; Hong, S. H.; Mirkin, C. A. *Science* **1999**, *283*, 661.
- (4) Lee, K. B.; Park, S. J.; Mirkin, C. A.; Smith, J. C.; Mirksich, M. *Science* **2002**, *295*, 1702.
- (5) Clausen-Schaumann, H.; Grandbois, M.; Gaub, H. E. *Adv. Mater.* **1998**, *10*, 949.
- (6) Tinazli, A.; Piehler, J.; Beuttler, M.; Guckenberger, R.; Tampe, R. *Nat. Nanotechnol.* **2007**, *2*, 220.
- (7) Staii, C.; Wood, D. W.; Scoles, G. J. *Am. Chem. Soc.* **2008**, *130*, 640.
- (8) Kufer, S. K.; Puchner, E. M.; Gump, H.; Liedl, T.; Gaub, H. E. *Science* **2008**, *319*, 594.
- (9) Binnig, G.; Quate, C. F.; Gerber, C. *Phys. Rev. Lett.* **1986**, *56*, 930.
- (10) Kufer, S. K.; Strackharn, M.; Stahl, S. W.; Gump, H.; Puchner, E. M.; Gaub, H. E. *Nat. Nanotechnol.* **2009**, *4*, 45.
- (11) Puchner, E. M.; Kufer, S. K.; Strackharn, M.; Stahl, S. W.; Gaub, H. E. *Nano Lett.* **2008**, *8*, 3692.
- (12) Cordes, T.; Strackharn, M.; Stahl, S. W.; Summerer, W.; Steinhauer, C.; Forthmann, C.; Puchner, E. M.; Vogelsang, J.; Gaub, H. E.; Tinnefeld, P. *Nano Lett.* **2010**, *10*, 645.
- (13) Strackharn, M.; Stahl, S. W.; Puchner, E. M.; Gaub, H. E. *Nano Lett.* **2012**, *12*, 2425.
- (14) Strackharn, M.; Stahl, S. W.; Severin, P. M.; Nicolaus, T.; Gaub, H. E. *ChemPhysChem* **2012**, *13*, 914.
- (15) Christy, B.; Nathans, D. *Proc. Natl. Acad. Sci. U.S.A.* **1989**, *86*, 8737.
- (16) Heim, R.; Cubitt, A. B.; Tsien, R. Y. *Nature* **1995**, *373*, 663.
- (17) Pedelacq, J. D.; Cabantous, S.; Tran, T.; Terwilliger, T. C.; Waldo, G. S. *Nat. Biotechnol.* **2006**, *24*, 79.
- (18) Zahnd, C.; Spinelli, S.; Luginbuhl, B.; Amstutz, P.; Cambillau, C.; Pluckthun, A. *J. Biol. Chem.* **2004**, *279*, 18870.
- (19) Morfill, J.; Blank, K.; Zahnd, C.; Luginbuhl, B.; Kuhner, F.; Gottschalk, K. E.; Pluckthun, A.; Gaub, H. E. *Biophys. J.* **2007**, *93*, 3583.
- (20) Greisman, H. A.; Pabo, C. O. *Science* **1997**, *275*, 657.
- (21) Kim, J. S.; Pabo, C. O. *Proc. Natl. Acad. Sci. U.S.A.* **1998**, *95*, 2812.
- (22) Gerber, D.; Maerkl, S. J.; Quake, S. R. *Nat. Methods* **2009**, *6*, 71.
- (23) Wang, Y.; Oyokawa, S.; Han, S. W.; Huang, W.; Ikebukuro, K.; Nakamura, C.; Miyake, J. *NanoBiotechnology* **2006**, *2*, 87.
- (24) Lv, S.; Dudek, D. M.; Cao, Y.; Balamurali, M. M.; Gosline, J.; Li, H. *Nature* **2010**, *465*, 69.
- (25) Myong, S.; Rasnik, I.; Joo, C.; Lohman, T. M.; Ha, T. *Nature* **2005**, *437*, 1321.
- (26) The pattern we used shows a traffic light man as it was used in eastern Germany. After the reunification it mostly disappeared from the streets, but currently it can be found again in German cities.
- (27) Funatsu, T.; Harada, Y.; Tokunaga, M.; Saito, K.; Yanagida, T. *Nature* **1995**, *374*, 555.
- (28) Dietz, H.; Rief, M. *Proc. Natl. Acad. Sci. U.S.A.* **2004**, *101*, 16192.
- (29) Korlach, J.; Marks, P. J.; Cicero, R. L.; Gray, J. J.; Murphy, D. L.; Roitman, D. B.; Pham, T. T.; Otto, G. A.; Foquet, M.; Turner, S. W. *Proc. Natl. Acad. Sci. U.S.A.* **2008**, *105*, 1176.
- (30) Bayer, E. A.; Shimon, L. J.; Shoham, Y.; Lamed, R. *J. Struct. Biol.* **1998**, *124*, 221.

(31) Zouni, A.; Witt, H. T.; Kern, J.; Fromme, P.; Krauss, N.; Saenger, W.; Orth, P. *Nature* **2001**, *409*, 739.

(32) Chen, W. W.; Niepel, M.; Sorger, P. K. *Genes Dev.* **2010**, *24*, 1861.

(33) Weitz, M.; Simmel, F. C. *Transcription* **2012**, *3*, 87.

(34) Kim, J.; Winfree, E. *Mol. Syst. Biol.* **2011**, *7*, 465.

Supporting Information

Nanoscale Arrangement of Proteins by Single-Molecule Cut&Paste

Mathias Strackharn[‡], Diana A. Pippig^{*,‡}, Philipp Meyer, Stefan W. Stahl[†], Hermann E. Gaub

Center for Nanoscience and Department of Physics, University of Munich, Amalienstraße 54, 80799 Munich, Germany

[†] Center for Integrated Protein Science (CIPSM), Munich, Germany

*diana.pippig@physik.uni-muenchen.de

[‡]These authors contributed equally.

The experiments described in the manuscript were performed on an AFM/TIRFM hybrid, the details of which may be found in [1]. This supporting information specifies methods and materials that are relevant for the conduction of the measurements discussed in the main text.

AFM Measurements

A custom built AFM head and an Asylum Research MFP3D controller (Asylum Research, Santa Barbara, USA), which provides ACD and DAC channels as well as a DSP board for setting up feedback loops were used. Software for the automated control of the AFM head and xy-piezos during the SMCP experiments was programmed in Igor Pro (Wave Metrics, Lake Oswego, USA). MLCT-AUHW levers (Bruker, Camarillo, USA) were chemically modified (further below) and calibrated in solution using the equipartition theorem [2],[3]. Pulling velocities were set to 2 $\mu\text{m/s}$ in the depot and 0.2 $\mu\text{m/s}$ in the target area. The positioning feedback accuracy is ± 3 nm. However, long term deviations may arise due to thermal drift. Typical times for one Cut & Paste cycle were in these experiments approximately 3 s.

TIRF Microscopy

The fluorescence microscope of the hybrid instrument excites the sample through the objective in total internal reflection mode. A 100x/1.49 oil immersion objective (CFI Apochromat TIRF, Nikon, Japan) was employed. Blue excitation for monitoring GFP fluorescence was achieved with a fiber-coupled 473 nm DPSS laser (CIEL, Laser Quantum, Cheshire, UK). The corresponding filter set consists of a Chroma z 470/10, a Chroma z 470 RDC and a Chroma HQ 525/50. Cy5 fluorophores were excited with a fiber-coupled 637 nm diode laser (iBeam smart, TOPTICA, München, Germany). Here the filter set was made up of a BrightLine HC 615/45, a Raman RazorEdge 633 RS, and a Chroma ET 685/70. All filters were purchased from AHF (Tübingen, Germany). Images

were recorded with a back-illuminated EMCCD camera (DU-860D, Andor, Belfast, Ireland) in frame transfer mode with 1 MHz readout rate at a frame rate of 10 Hz. The gain was set to 200. The camera was water cooled and operated at -75 °C.

Preparation of the C11L34 Single Chain Antibody Fragment

The C11L34 single chain antibody fragment was prepared as described in [4]. The scFv construct harbored a C-terminal His tag followed by a Cys to allow for site-specific immobilization and was obtained by periplasmic expression in *E. coli* SB536. C11L34 was purified by Ni²⁺ and immobilized antigen affinity chromatography according to standard protocols. The concentration was adjusted to 1.6 mg/ml in a storage buffer containing 50 mM sodium phosphate, pH 7.2, 50 mM NaCl and 10 mM EDTA.

Preparation of the GCN4-GFP-Zinc Finger Fusion Construct

A fusion protein construct consisting of an N-terminal GCN4(7P14P)-tag [4] (RMKQLEPKVEELLPKNYHLENEVARLKKLVGER) and the six Zinc Finger peptide Zif268/NRE (with an RQKDGERP linker sequence between the Zif268 and NRE moieties) was designed according to [5]. All construct fragments were amplified from synthetic templates (Mr.Gene or Geneart, Lifetechnologies, Paisley, UK). GCN4 was cloned into pET28a between NcoI and NdeI restriction sites. The original sequence coding for the Thrombin cleavage site in pET28a was replaced by one coding for the TEV-protease recognition site. Zif268/NRE was inserted subsequently between NdeI and NotI sites. A C-terminal ybbR-tag (DSLEFIASKLA) [6] is flanking the Zinc Finger region. The whole construct was subcloned into pGEX6P2 by means of BamHI and XhoI sites. Superfolder GFP [7] followed by a SGSG linker was inserted between the TEV

coding site and Zif268/NRE by sequence and ligation independent cloning [8]. The resulting fusion protein (GCN4-TEV-sfGFP-Zif268/NRE-ybbR) harbored a GST-tag and was expressed in *E.coli* BL21 DE3 cells. For this, one liter of SB medium was inoculated with 10 ml of an overnight culture and grown at 37°C. When an OD₆₀₀ of 0.7 had been reached, over night expression at 18°C was induced by adding 0.25mM IPTG.

Cells were lysed in 50mM Tris HCl pH 7.5, 300 mM NaCl, 2mM DTT, 5% Glycerol, 10µM ZnCl₂ by a French pressure cell press. The GCN4-GFP-Zinc Finger construct was obtained in the soluble fraction and purified by Glutathione affinity chromatography on GST Trap columns (GE Healthcare, Freiburg, Germany). After over night incubation with PreScission protease the GST-tag was removed and the protein further purified by Heparin cation exchange chromatography (HiTrap Heparin, GE Healthcare, Freiburg, Germany). The purified fusion protein was dialyzed into storage buffer (50mM Tris HCl pH7.5, 150mM NaCl, 2mM DTT, 10µM ZnCl₂, 5% Glycerol), stored at -80°C and had a final concentration of 10µM.

Preparation of Cantilevers

Cantilevers were oxidized in a UV-ozone cleaner (UVOH 150 LAB, FHR Anlagenbau GmbH, Ottendorf-Okrilla, Germany) and silanized by soaking for 2 min in (3-Glycidoxypropyl)trimethoxysilane (ABCR, Karlsruhe, Germany). Subsequently they were washed in toluene, 2-propanol and ddH₂O and dried at 80 °C for 40 min. After incubating the cantilever in 10 mg/ml aminodextrane (D1860, Invitrogen, Carlsbad, USA) in a sodium borate buffer (pH 8.5), a heterobifunctional PEG crosslinker [9] with

N-hydroxy succinimide and maleimide groups (MW 5000, Rapp Polymere, Tübingen, Germany) was then applied for 1 h at 30 mM and then the C11L34 antibody fragments were bound at 8 °C to the lever during 4 h. Finally the cantilever was washed with PBS.

Preparation of Cover Glass Slips

Cover glasses were sonicated in 50% (v/v) 2-propanol in ddH₂O for 15 min and oxidized in solution of 50% (v/v) hydrogen peroxide (30%) and sulfuric acid for 30 min. They were then washed in ddH₂O and dried in a nitrogen stream, silanized by soaking for 1 h in (3-Glycidoxypropyl)trimethoxysilane (ABCR, Karlsruhe, Germany). Subsequently they were washed twice in 2-propanol and ddH₂O and dried at 80 °C for 40 min. After this they were incubated in 10 mg/ml aminodextrane (D1860, Invitrogen, Carlsbad, USA) in a sodium borate buffer (pH 8.5), a heterobifunctional PEG crosslinker with N-hydroxy succinimide and maleimide groups (MW 5000, Rapp Polymere, Tübingen, Germany) was then applied for 1 h at 30 mM. Depot and Target DNA was reduced with TCEP and subsequently purified by ethanol precipitation. DNA pellets were dissolved in a phosphate buffer (pH 7.2, 50 mM NaCl, 10 mM EDTA). Target DNA was mixed with 10 % of a thiolated oligomer with the Zinc Finger recognition sequence. This ensures that a fusion protein without DNA, which might during the experiment attach to the cantilever, does not block antibody binding sites. A microfluidics system was now fixed on the cover glass, and the depot or the target oligomers were pumped through the channels for 1 h. Subsequently both channels were flushed with PBS. Zinc Finger A and B oligomers were mixed to 500 nM in a 1:1 ratio in PBS, heated to 80 °C during 10 min and then

cooled at 4 °C for 90 min. The fusion protein was added to a final concentration of 500 nM and allowed to bind to the DNA during additional 90 min. The protein-DNA solution was then flowed through the Depot channel for 90 min. Subsequently the channel was rinsed again with PBS and the microfluidics system was removed.

SMC&P Experiment

Patterns were written in 900 transfer cycles. Pulling speeds of the cantilever at the individual transfer steps were chosen to optimize the rupture force distribution of the respective bonds (Fig. S1), which depend in a first order approximation logarithmically on the force loading rate [10]. The pulling speed in the depot was set to 2 $\mu\text{m/s}$ and in the target to 0.2 $\mu\text{m/s}$.

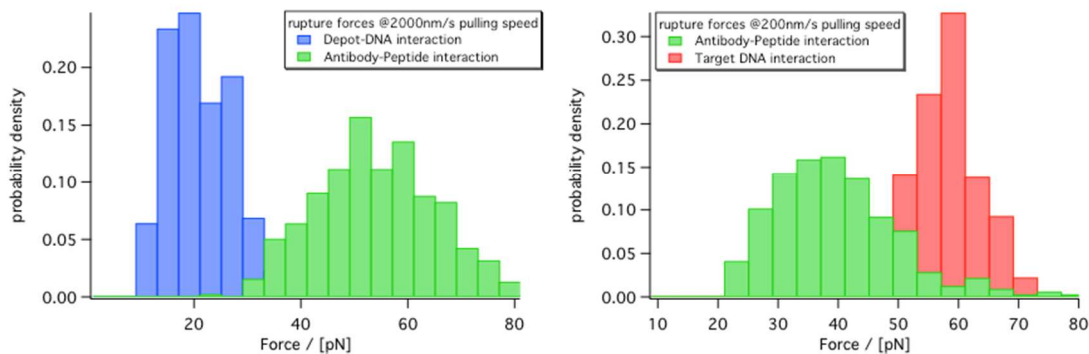


Figure S1. Histograms of the rupture force distribution of the involved unbinding steps in the depot area (left) and the target area (right).

The functionalization density of the cantilever, depot and target region was adjusted such that on average 1.8 protein:DNA complexes were transferred per cycle (Fig. S2).

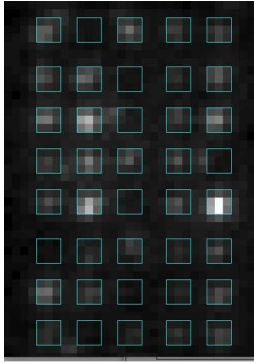


Figure S2. In order to determine the typical transfer efficiency for the functionalization densities that were used in the protein arrangement experiments, a regular pattern with 40 transfer cycles was assembled. The number of transferred molecules was obtained by counting the number of Cy5 bleaching steps per spot. On average about 2 molecules were transferred per cycle.

Oligomer Sequences

thiolated depot oligomer

5' SH - TTT TTT CAT GCA AGT AGC TAT TCG AAC TAT AGC TTA AGG ACG
TCA A

thiolated target oligomer

5' CAT GCA AGT AGC TAT TCG AAC TAT AGC TTA AGG ACG TCA ATT TTT –
SH

Zinc Finger A oligomer

5' Cy5
TTTGACGTCCTTAAGCTATAGTTCGAATAGCTACTTGCAATGTTTTTTTTTTTTTT
TTTTT TTTTTTTTTTTTTTCTGCAAGGGTTCAGGCGTGGGCGGTAAG

Zinc Finger B oligomer

5' CTTACCGCCCACGC C TGAACCCTTGCAGA

References

1. Gump, H., et al., *Ultrastable combined atomic force and total internal reflection fluorescence microscope [corrected]*. The Review of scientific instruments, 2009. **80**(6): p. 063704.
2. Florin, E., *Sensing specific molecular interactions with the atomic force microscope*. Biosensors and Bioelectronics, 1995. **10**(9-10): p. 895-901.
3. Butt, H.J. and M. Jaschke, *Calculation of thermal noise in atomic-force microscopy*. Nanotechnology, 1995. **6**(1): p. 1-7.
4. Morfill, J., et al., *Affinity-matured recombinant antibody fragments analyzed by single-molecule force spectroscopy*. Biophysical journal, 2007. **93**(10): p. 3583-90.
5. Kim, J.S. and C.O. Pabo, *Getting a handhold on DNA: design of poly-zinc finger proteins with femtomolar dissociation constants*. Proceedings of the National Academy of Sciences of the United States of America, 1998. **95**(6): p. 2812-7.
6. Yin, J., et al., *Site-specific protein labeling by Sfp phosphotransferase*. Nature protocols, 2006. **1**(1): p. 280-5.
7. Pedelacq, J.D., et al., *Engineering and characterization of a superfolder green fluorescent protein*. Nature biotechnology, 2006. **24**(1): p. 79-88.
8. Bryksin, A.V. and I. Matsumura, *Overlap extension PCR cloning: a simple and reliable way to create recombinant plasmids*. BioTechniques, 2010. **48**(6): p. 463-5.
9. Celik, E. and V.T. Moy, *Nonspecific interactions in AFM force spectroscopy measurements*. J Mol Recognit, 2012. **25**(1): p. 53-6.
10. Evans, E. and K. Ritchie, *Dynamic strength of molecular adhesion bonds*. Biophysical journal, 1997. **72**(4): p. 1541-55.